

Cite this: *RSC Adv.*, 2018, 8, 9311

Polymeric ionic liquid gels composed of hydrophilic and hydrophobic units for high adsorption selectivity of perrhenate†

Dong Han,^{‡a} Xingxiao Li,^{‡a} Yu Cui,^a Xin Yang,^a Xibang Chen,^a Ling Xu,^{bc} Jing Peng,^{*a} Jiuqiang Li^a and Maolin Zhai^{ID}^{*a}

The removal of TcO_4^- from aqueous solutions has attracted more and more attention recently, and ReO_4^- has been widely used as its natural analog. In this work, polymeric ionic liquid gel adsorbents, $\text{PC}_2\text{-C}_{12}\text{vimBr}$, with high adsorption capacity and selectivity towards ReO_4^- were synthesized by radiation-induced polymerization and crosslinking. $\text{PC}_2\text{-C}_{12}\text{vimBr}$ was composed of two monomers: a hydrophobic unit, 1-vinyl-3-dodecylimidazolium bromide for high selectivity, and a hydrophilic unit, 1-vinyl-3-ethylimidazolium bromide for improved kinetics. A gel fraction up to 90% could be achieved under 40 kGy with varied monomer ratios. The adsorption of $\text{PC}_2\text{-C}_{12}\text{vimBr}$ gels for ReO_4^- was evaluated by batch adsorption. The $\text{PC}_2\text{-C}_{12}\text{vimBr}$ gel containing 20 mol% hydrophilic unit (named $\text{PC}_2\text{-C}_{12}\text{vimBr-A}$) could significantly improve the adsorption kinetics, which had an equilibrium time of ca. 24 h. The adsorption capacity obtained from the Langmuir model was 559 mg g^{-1} (Re/gel). The selective factor against NO_3^- was 33.4 ± 1.9 , which was more than 10 times higher than that of PC_2vimBr , and it could maintain ReO_4^- uptake as high as 100 mg g^{-1} in $0.5 \text{ mol kg}^{-1} \text{ HNO}_3$. The ΔH^\ominus and ΔS^\ominus of the $\text{NO}_3^-/\text{ReO}_4^-$ ion-exchange reaction of $\text{PC}_2\text{-C}_{12}\text{vimNO}_3\text{-A}$ were $-16.9 \text{ kJ mol}^{-1}$ and $29 \text{ J mol}^{-1} \text{ K}^{-1}$, respectively, indicating physical adsorption. The adsorption mechanism of ReO_4^- onto $\text{PC}_2\text{-C}_{12}\text{vimBr-A}$ gel was ion-exchange, and it could be recovered using $5.4 \text{ mol kg}^{-1} \text{ HNO}_3$.

Received 27th January 2018
Accepted 26th February 2018

DOI: 10.1039/c8ra00838h

rsc.li/rsc-advances

1. Introduction

Technetium (Tc) is an artificial element, and all its isotopes are radioactive. A large amount of ^{99}Tc is produced from nuclear plants nowadays, and exists in high-level liquid waste. Since Tc is hazardous and has high mobility in the environment, and it may affect the geological disposal of other radioactive nuclei, the removal of Tc from aqueous solutions has attracted more and more attention recently.¹ And because of the radioactivity of Tc, it is not allowed to be handled in the normal lab, and rhenium (Re) has been extensively used as its analog owing to their similar chemistry properties.^{1–3}

Tc mainly exists in the form of TcO_4^- in the high-level waste.⁴ Many kinds of method to remove TcO_4^- and ReO_4^- have been

investigated in recent years, including the reductive immobilization of TcO_4^- or ReO_4^- by Fe(0) ^{5,6} and the direct adsorption by adsorbents.^{7–10} Comparing to the reductive method, the adsorption takes the advantage of high adsorption capacity and the reusability of the adsorbents.

Most adsorbents towards TcO_4^- and ReO_4^- depended on ion-exchange. MOFs,^{11–14} carbon materials,^{15–18} and organic adsorbents have been employed as the adsorbents. Organic adsorbents including resins,^{19,20} grafted materials^{21,22} and gels^{23,24} take the advantage of high adsorption capacities and easy design and synthesis. Quaternary ammonium^{19,23} including pyridinium^{25,26} and imidazolium^{3,21,27} have been used as the functional groups in many ion-exchange adsorbents.¹⁹ For the quaternary ammonium, alkyl has been widely used as the group on the quaternary N atom, including ethyl, propyl, butyl, pentyl, hexyl *etc.*^{28,29} And it was found that longer alkyl chain in quaternary ammonium may bring higher selectivity towards ReO_4^- .²⁸

However, adsorbents depending on ion-exchange would be influenced by the other anions in the solution as competitors, and a large amount of NO_3^- exists in the high-level liquid waste. So it is very important to develop adsorbents with high selectivities towards TcO_4^- or ReO_4^- . Wang *et al.* reported a TcO_4^- adsorbent, NDTB-1, with an adsorption capacity of 162.2 mg g^{-1} and a maximum distribution coefficient K_d of

^aBeijing National Laboratory for Molecular Sciences, Radiochemistry and Radiation Chemistry Key Laboratory of Fundamental Science, The Key Laboratory of Polymer Chemistry and Physics of the Ministry of Education, College of Chemistry and Molecular Engineering, Peking University, Beijing 100871, China. E-mail: jpeng@pku.edu.cn; mlzhai@pku.edu.cn

^bState Key Laboratory of Molecular Vaccinology and Molecular Diagnostics, School of Public Health, Xiamen University, Xiamen, Fujian 161102, China

^cPeking University Shenzhen Institute, Shenzhen 518057, China

† Electronic supplementary information (ESI) available: IR, TGA, EA, and XPS of $\text{PC}_2\text{-C}_{12}\text{vimBr}$. See DOI: 10.1039/c8ra00838h

‡ These authors contributed equally to this work.

$1.0534 \times 10^4 \text{ mL g}^{-1}$.¹⁰ Shu *et al.* developed a surface ion-imprinted magnetic microsphere ReO_4^- adsorbent containing imidazolium groups with an adsorption capacity of 62.8 mg g^{-1} and a Langmuir constant of 1.35 L mg^{-1} .³

On the other hand, some of the reported excellent adsorbents contain metal elements, *e.g.* Ag in SCU-100,¹³ which may result in the increase of radioactive wastes. Adsorbents composed of only C, H, N, O may avoid the secondary radioactive waste since they follow the CHON principle.^{30,31} Organic adsorbents such as polymeric ionic liquids may meet this requirement.

Polymeric ionic liquid is a kind of polymer which contains ionic liquid units, and they have attracted much attention in many fields, such as polyelectrolytes, polymeric surfactants, anion sensitive smart materials,^{32,33} gas separation membranes,³⁴ and also ion-exchange adsorbents.³⁵ Recently we reported a polymeric ionic liquid gel ReO_4^- adsorbent with high adsorption capacity of 865 mg g^{-1} , but the selectivity is not high enough, and we proposed that hydrophobic polycations might have higher selectivity towards ReO_4^- .²⁴ Polymers with both hydrophilic and hydrophobic segments have been reported with interesting self-assembling behaviors³⁶ or as proton conductive membranes.³⁷ Considering the advantages of combination of the hydrophilic and the hydrophobic segments in polymers, *i.e.* the hydrophobic one is favour for higher adsorption selectivity towards ReO_4^- and the hydrophilic one is better for adsorption kinetics, we herein developed a polymeric ionic liquid gel adsorbent, $\text{PC}_2\text{-C}_{12}\text{vimBr}$, with high adsorption capacity and selectivity, which was synthesized easily by radiation-induced polymerization and crosslinking of 1-vinyl-3-alkylimidazolium. Considering longer alkyl chain on the quaternary N atom can increase the hydrophobicity of gels, which may result in higher adsorption selectivity towards ReO_4^- , a hydrophobic unit, 1-vinyl-3-dodecylimidazolium bromide ($\text{C}_{12}\text{vimBr}$) was chosen to improve the selectivity. On the other hand, a hydrophilic unit, 1-vinyl-3-ethylimidazolium bromide (C_2vimBr), was chosen to improve the adsorption kinetics of ReO_4^- in aqueous solution. A series of $\text{PC}_2\text{-C}_{12}\text{vimBr}$ gels with different molar ratio of hydrophobic and hydrophilic units were synthesized and characterized, and their adsorption kinetics towards ReO_4^- were investigated. Then the adsorption isotherm, selectivity and mechanism of $\text{PC}_2\text{-C}_{12}\text{vimBr}$ gel were investigated in detail.

2. Experimental

2.1 Materials

C_2vimBr and $\text{C}_{12}\text{vimBr}$ monomers were purchased from Lanzhou Greenchem ILS, LICP. CAS., dried in vacuum to remove the residual solvent. 3,3'-Divinyl-1,1'-(1,6-hexanediyl) diimidazolium dibromide ($\text{C}_6\text{vim}_2\text{Br}_2$) was easily synthesized as we reported before.²⁴ 1,6-Dibromohexane was purchased from J&K, and 1-vinylimidazole was provided by TCI. KReO_4 was obtained from Alfa Aesar. Re standard solution was provided by NCS Testing Technology Co., Ltd. Some HNO_3 mother solutions with certain concentrations were prepared from GR HNO_3 (Xilong Chemical Co., Ltd.) and titrated. Other chemicals were analytical-grade reagents. Deionized water was used throughout the experiments.

2.2 Preparation and characterization of $\text{PC}_2\text{-C}_{12}\text{vimBr}$ gels

Preparation of $\text{PC}_2\text{-C}_{12}\text{vimBr}$ gels. C_2vimBr , $\text{C}_{12}\text{vimBr}$ and $\text{C}_6\text{vim}_2\text{Br}_2$ were mixed into an aqueous solution and added into a glass test tube. It was then γ -irradiated at a dose rate of *ca.* 40 Gy min^{-1} to a dose of 40 kGy by the ^{60}Co source, which was calibrated by Fricke dosimeter. The solution became into a white opaque gel after radiation. The concentration of $\text{C}_6\text{vim}_2\text{Br}_2$ crosslinker was set as 0.05 M . The total concentration of C_2vimBr and $\text{C}_{12}\text{vimBr}$ monomers was 1 M , and their feed ratios and the short names of the resulted gels were shown in Table 1.

The resulted gels were cut into round pieces with a thickness of *ca.* 3 mm , and then every round piece was evenly cut into 4 sector pieces for further usage. The gels were immersed into excess ethanol for more than 6 times (at least 1 day for every time) to remove the sol part, and was subsequently put into excess water for more than 4 times. Then the gels were dried under 60°C for more than 2 days to a constant weight. Gel fraction (GF) and equilibrium degree of swelling (EDS) were measured by gravimetry.

GF is defined as:

$$\text{GF (\%)} = w_g/w_0 \times 100 \quad (1)$$

where w_g is the weight of dry gel after removing the sol part, and w_0 is the initial weight of dry gel.

EDS is defined as:

$$\text{EDS} = w_e/w_d \quad (2)$$

where w_d is the dry weight of the gel and w_e is the weight of the swelled gel after swelling equilibrium.

Characterization of $\text{PC}_2\text{-C}_{12}\text{vimBr}$ gels. IR spectra were obtained from Nicolet iS50. XPS was performed on Axis Ultra (Kratos Analytical) and B.E. were calibrated by C 1s hydrocarbon peak as 284.80 eV . Elemental Analysis (EA) was performed on Elementar Vario EL CUBE. SEM images were measured using Nova NanoSEM 430, and the samples were prepared by freeze-drying from gels well swelled in water.

2.3 Adsorption of ReO_4^- onto $\text{PC}_2\text{-C}_{12}\text{vimBr}$ gels

The mother solution of Re was prepared from deionized water and KReO_4 . Inductively coupled plasma atomic emission spectroscopy (ICP-AES, Prodigy) was used to measure the Re concentration, and the relative error of Re concentration was estimated as 2%.

Table 1 Feed concentrations of monomers and the resulted gels

Feed concentrations (M)			Names of the resulted gels
C_2vimBr	$\text{C}_{12}\text{vimBr}$	$\text{C}_6\text{vim}_2\text{Br}_2$	
0	1	0.05	$\text{PC}_{12}\text{vimBr}$
0.2	0.8	0.05	$\text{PC}_2\text{-C}_{12}\text{vimBr-A}$
0.4	0.6	0.05	$\text{PC}_2\text{-C}_{12}\text{vimBr-B}$
0.6	0.4	0.05	$\text{PC}_2\text{-C}_{12}\text{vimBr-C}$
0.8	0.2	0.05	$\text{PC}_2\text{-C}_{12}\text{vimBr-D}$



Typically, an adsorption experiment was performed as following: a piece of gel was immersed into a Re solution, the mass ratio of the gel to the solution was 1 mg gel per 1 g solution. The system was shaken in a shaker at 25 °C for *ca.* 2 days to reach equilibrium, and the concentration of Re in the resulted solution was measured by ICP-AES.

The Re uptake, q , was calculated as following:

$$q = \frac{(c_0 - c) \times m_s}{m_g} \quad (3)$$

where c_0 is the concentration of Re before adsorption, and c is the concentration of Re after adsorption, while m_s is the mass of the solution, and m_g is the mass of the dry gel.

Adsorption kinetics. Since the gels were composed of imidazolium units with different molecular weights, sector pieces of gels with the similar sizes before washing were used to compare their adsorption kinetics. The gels were *ca.* 20–40 mg, and the corresponding m_s was constant at 50 g. 100 μ L of solution was taken out from the system at a certain time and diluted to measure the Re concentration.

Adsorption isotherms and selectivity. For adsorption isotherms, a series of q and c were measured with varied c_0 . For adsorption selectivity, NO_3^- and Br^- , which were from HNO_3 and NaBr respectively, were chosen as anion competitors.

In the competitive adsorption against NO_3^- , the anion of the gel were exchanged into NO_3^- before the adsorption, forming $\text{PC}_2\text{-C}_{12}\text{vimNO}_3\text{-A}$. In detail, $\text{PC}_2\text{-C}_{12}\text{vimBr-A}$ was immersed into excess *ca.* 1.5 M HNO_3 to equilibrium for 2 times, then into water for 3 times and dried. XPS and IR were performed to confirm the formation of $\text{PC}_2\text{-C}_{12}\text{vimNO}_3\text{-A}$ (Fig. S1†).

The selective factor (SF) was used to evaluate the selectivities toward ReO_4^- against NO_3^- and Br^- . SF was defined as:³⁶

$$\text{SF} = \frac{q(\text{Re}) \times c(\text{competitor})}{q(\text{competitor}) \times c(\text{Re})} \quad (4)$$

where q is the uptake of the corresponding ion, and should be converted into the same unit (mmol g^{-1}). And c is the remained

concentration (converted into mol kg^{-1}) of the corresponding ion at equilibrium. Thus, SF is a dimensionless number and suitable for the comparison between different adsorbents.

The SF of PC_2vimBr , a Re adsorbent reported in our previous work,²⁴ towards ReO_4^- against NO_3^- was measured by the same procedure.

For the selective adsorption in ethanol–water mix solvent, the concentration of HNO_3 was 0.05 mol kg^{-1} .

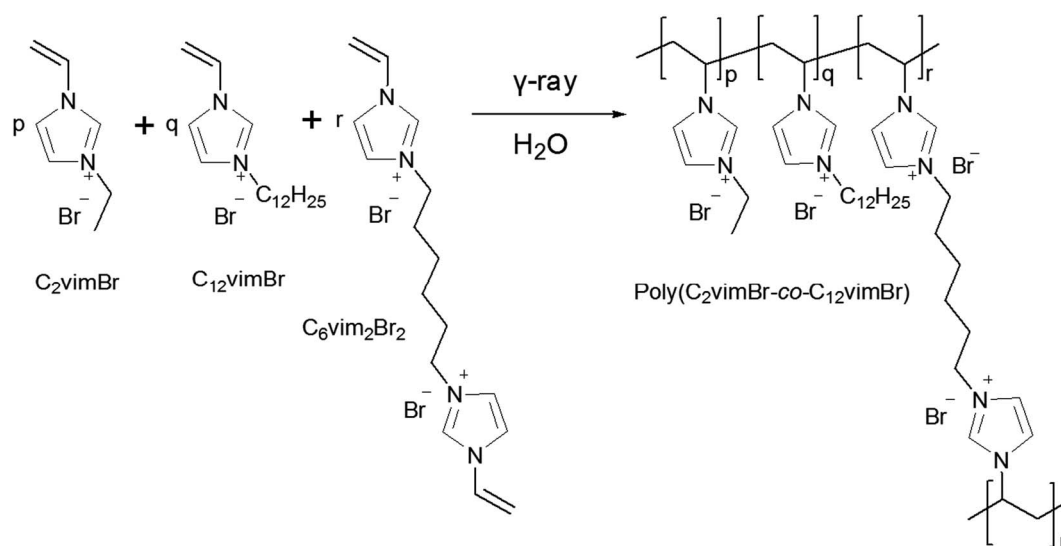
Adsorption thermodynamics. In the solution, the c_0 was 700 ppm, and the concentration of HNO_3 was 0.05 mol kg^{-1} . The phase ratio was 1 mg gel per 1 g solution, and the solution was more than 60 g in each system. The system was shaken in a shaker for more than 2 days at each temperature, then 100 μ L of solution was taken to measure the c . Less than 1% of the solution was taken out for measurement during the whole experiment to avoid the influence by the change of the solution volume.

Adsorption cycles. In the first cycle, a piece of $\text{PC}_2\text{-C}_{12}\text{vimBr-A}$ was used to adsorb ReO_4^- ($c_0 = 1176$ ppm) and became $\text{PC}_2\text{-C}_{12}\text{vimReO}_4\text{-A}$ after the adsorption. Then $\text{PC}_2\text{-C}_{12}\text{vimReO}_4\text{-A}$ was desorbed by 5.40 mol kg^{-1} HNO_3 (1 g per mg $\text{PC}_2\text{-C}_{12}\text{vimBr-A}$), and the solution was collected to measure the amount of desorbed Re. After that it was further immersed into 5.40 mol kg^{-1} HNO_3 for another time and then into water for 3 times to get rid of the residual ReO_4^- and HNO_3 . Thus $\text{PC}_2\text{-C}_{12}\text{vimNO}_3\text{-A}$ was formed and used for the next cycle. After 4 cycles, IR and XPS were performed to the resulted $\text{PC}_2\text{-C}_{12}\text{vimNO}_3\text{-A}$ to confirm the desorption, as well as to the $\text{PC}_2\text{-C}_{12}\text{vimReO}_4\text{-A}$ in the first cycle to confirm the adsorption.

3. Result and discussion

3.1 Preparation and characterization of $\text{PC}_2\text{-C}_{12}\text{vimBr}$ gels

Radiation-induced polymerization and crosslinking is a green and clean method widely used to prepare gels,³⁷ and it has been proved to be effective for the preparation of poly ionic liquid gels in our previous works.²⁴ The synthesis of $\text{PC}_2\text{-C}_{12}\text{vimBr}$ gels



Scheme 1



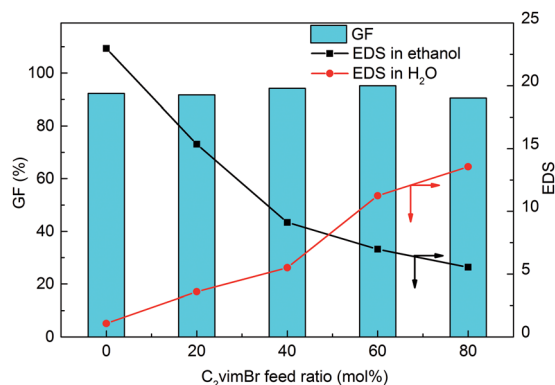


Fig. 1 GF and EDS of the PC₁₂vimBr gel and PC₂-C₁₂vimBr gels.

was illustrated in Scheme 1, and the GF and the EDS of PC₂-C₁₂vimBr gels were shown in Fig. 1.

The GFs of all PC₂-C₁₂vimBr gels with different compositions synthesized under 40 kGy were above 90%, which indicated that γ -radiation-induced polymerization and crosslinking was suitable and effective for this system. IR, TGA, EA, and XPS were performed to confirm the composition and structure of the resultant gels, and the results were shown in the ESI (Fig. S2–S4 and Table S1†).

PC₁₂vimBr, which had no C₂vimBr units, nearly did not swell in water, but it swelled well in ethanol. The EDS of PC₂-C₁₂vimBr gels in water increased with the increasing C₂vimBr content, while the EDS in ethanol decreased. Since all the five gels had the same crosslinker content, the differences of the EDS of the gels in water and in ethanol were due to the different contents of the short-chain C₂vimBr units and the long-chain C₁₂vimBr units, and the results reflected the hydrophilicities and hydrophobicities of the gels. The more C₂vimBr units the gel contains, the more hydrophilic it was, while the C₁₂vimBr units contributed to the hydrophobicity of the gel.

SEM images were taken from the xerogels prepared by freeze-drying of the corresponding gels swelled in water. SEM images of PC₂-C₁₂vimBr-A, PC₂-C₁₂vimBr-D and PC₁₂vimBr gel were shown in Fig. 2. Among the three samples, PC₂-C₁₂vimBr-D had the largest holes, and it was agreed with its highest EDS in water. PC₂-C₁₂vimBr-A, which had least C₂vimBr units among PC₂-C₁₂vimBr gels, also had small holes, while it could swell a little in water. In the image of PC₁₂vimBr, the section was rough and no hole could be observed. PC₁₂vimBr was relatively hydrophobic, and did not swell in water, while even a small

amount of C₂vimBr units could give the gels hydrophilicity and make them swell in water, which would improve their adsorption kinetics.

3.2 The adsorption kinetics of ReO₄[−] onto PC₂-C₁₂vimBr gels

PC₂-C₁₂vimBr gel had a cationic polymer network with Br[−] as exchangeable counteranion, so anions such as ReO₄[−] can be attracted easily by PC₂-C₁₂vimBr gel and then be adsorbed by anion-exchange. The adsorption kinetics of ReO₄[−] onto four PC₂-C₁₂vimBr gels were shown in Fig. 3a, and that of PC₁₂vimBr was shown in Fig. 3b.

For all the four PC₂-C₁₂vimBr gels, the kinetics had no significant difference. The adsorption equilibriums were achieved at *ca.* 24 h, which was similar to the equilibrium time of poly(4-vinylpyridine) resins.²⁹ However, PC₁₂vimBr shown a quite slow adsorption kinetics, and could not achieve equilibrium in even 3 months. This was due to the high hydrophobicity of PC₁₂vimBr, and as shown in Fig. 2c, it had no porous structure in water. On the other hand, as little as 20 mol% of the short-chain C₂vimBr units could improve the hydrophilicity of the gel, and further efficiently improve the adsorption kinetics. Upon 20 mol%, more C₂vimBr units did not show significant improvement to the adsorption kinetics. Since we introduced the long-chain C₁₂vimBr units aiming at improving the adsorption selectivity towards ReO₄[−] (the gels with lower C₁₂vimBr contents had lower adsorption selectivity towards ReO₄[−], see Fig. S5†), PC₂-C₁₂vimBr-A, which had the highest content of C₁₂vimBr units among the gels with suitable kinetics, was chosen for the further adsorption experiments.

3.3 The adsorption isotherms and selectivity of PC₂-C₁₂vimBr-A towards ReO₄[−]

The adsorption isotherms. The adsorption isotherms of ReO₄[−] onto PC₂-C₁₂vimBr-A was shown in Fig. 4.

The adsorption isotherms of ReO₄[−] onto PC₂-C₁₂vimBr-A agreed with the Langmuir model well:

$$q = q_m \times \frac{kc}{1 + kc} \quad (5)$$

where q_m is the adsorption capacity, and k is the Langmuir constant.

And it was fitted in the linear form:

$$\frac{c}{q} = \frac{c}{q_m} + \frac{1}{q_mk} \quad (6)$$

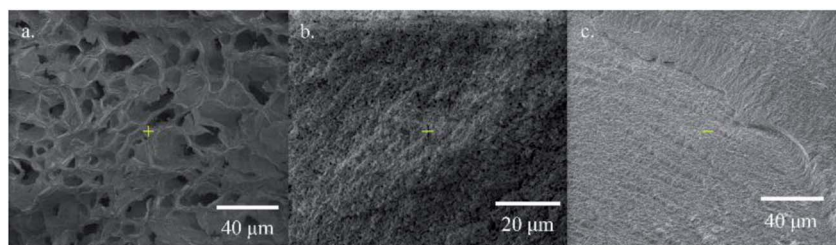


Fig. 2 SEM images of (a) PC₂-C₁₂vimBr-D, (b) PC₂-C₁₂vimBr-A, and (c) PC₁₂vimBr.



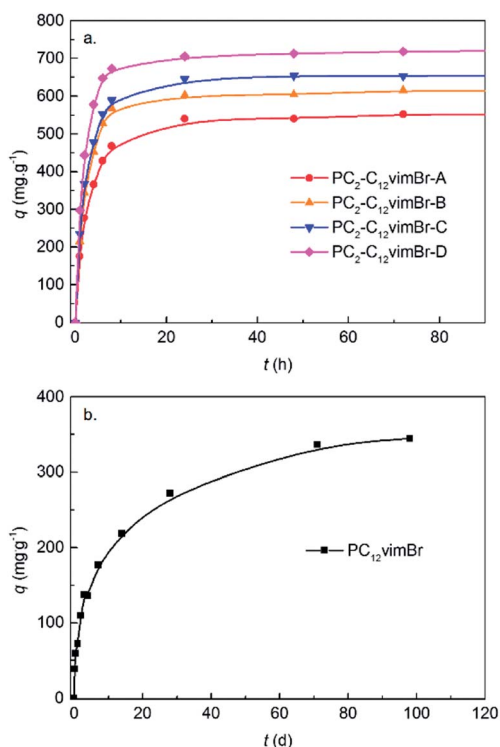


Fig. 3 Adsorption kinetics of ReO_4^- onto (a) $\text{PC}_2\text{-C}_{12}\text{vimBr}$ gels and (b) $\text{PC}_{12}\text{vimBr}$. The c_0 was 557 ppm.

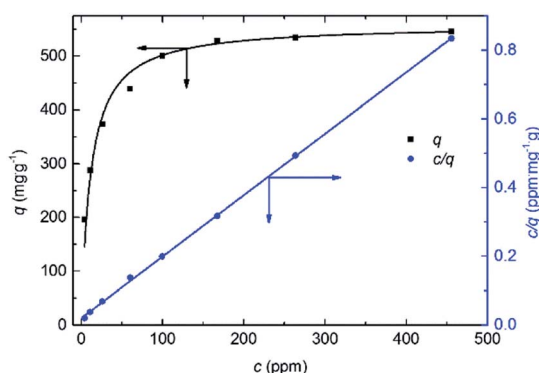


Fig. 4 Adsorption isotherms of ReO_4^- onto $\text{PC}_2\text{-C}_{12}\text{vimBr-A}$.

The parameters of fitting and the calculated q_m and k were shown in Table 2:

The q_m of Re onto $\text{PC}_2\text{-C}_{12}\text{vimBr-A}$ was 559 mg Re per g gel, which was equal to the theoretical value calculated from the N wt% in the EA of $\text{PC}_2\text{-C}_{12}\text{vimBr-A}$, assuming every imidazolium group could adsorb one ReO_4^- ion:

$$q_{\text{th}} = \frac{\text{wt}\%(N)}{M_w(N)} \times \frac{n(\text{imidazolium})}{n(N)} \times M_w(\text{Re})$$

$$= \frac{8.40\%}{14.0} \times \frac{1}{2} \times 186.2 \text{ g g}^{-1}$$

$$= 559 \text{ mg g}^{-1}$$

(7)

This result also supported that all imidazolium groups in $\text{PC}_2\text{-C}_{12}\text{vimBr-A}$ were utilized with a ratio to ReO_4^- of 1 : 1.

Since the long-chain unit $\text{C}_{12}\text{vimBr}$ has larger M_w than that of C_2vimBr , the q_m of $\text{PC}_2\text{-C}_{12}\text{vimBr-A}$ was lower than that of the Re adsorbent PC_2vimBr we reported before, which was 865 mg g^{-1} .²⁴ However, as a gel adsorbent, $\text{PC}_2\text{-C}_{12}\text{vimBr-A}$ was fully composed of functional groups without matrix, its adsorption capacity was higher than most of the Re adsorbents reported.^{3,10,16}

For the practical usage of Re/Tc adsorbents, the selectivity is more important than the adsorption capacities. Because in practical systems, TcO_4^- usually presences with competitors, e.g. HNO_3 in the PUREX.⁴ The results of the competitive adsorption against Br^- and NO_3^- were shown in Fig. 5.

As shown in Fig. 5, the q of Re decreased with the increasing concentration of the competitor in all the three curves, and it was due to the competition of NO_3^- or Br^- . SF should be a constant according to the Langmuir model, and was fluctuating around the average value among the investigated conditions. The average values of SF were listed in Table 3.

Comparing to $\text{PC}_2\text{vimNO}_3$, the adsorbent we previously reported,²⁴ $\text{PC}_2\text{-C}_{12}\text{vimNO}_3\text{-A}$ had an SF against NO_3^- more than 10 times higher than that of the former one, which illustrated its excellent selectivity towards ReO_4^- . Since few literatures about Re adsorbents have reported the SF between NO_3^- and ReO_4^- , it is a little difficult to compare the selectivities widely among these adsorbents, considering some reported quantities, e.g. distribution coefficient K_d or removal rate, are not only decided by the nature of the materials, but also by the experiment parameters such as the phase ratio of adsorbent/solution and the c_0 of Re. We estimated the SF towards ReO_4^- against NO_3^- of SCU-100, which is an excellent Re/Tc adsorbent reported recently with the highest K_d among inorganic Re adsorbents, from its adsorption capacity as 541 mg ReO_4^- per g SCU-100 and removal rate as 73% at 0.15 mM ReO_4^- and 15 mM NO_3^- with a phase ratio of 1 mL solution per 1 mg SCU-100.¹³

$$\text{SF} = \frac{q(\text{Re}) \times c(\text{competitor})}{q(\text{competitor}) \times c(\text{Re})}$$

$$= \frac{(73\% \times 0.15 \times 1/1) \text{ mmol g}^{-1} \times 15 \text{ mM}}{(541/250.2 - 73\% \times 0.15 \times 1/1) \text{ mmol g}^{-1} \times (27\% \times 0.15) \text{ mM}}$$

$$= 20$$

(8)

It was illustrated that the measured SF of $\text{PC}_2\text{-C}_{12}\text{vimNO}_3\text{-A}$ was higher than the estimated SF of SCU-100, i.e. $\text{PC}_2\text{-C}_{12}\text{vimNO}_3\text{-A}$ had better selectivity towards ReO_4^- . $\text{PC}_2\text{-C}_{12}\text{vimNO}_3\text{-A}$ could remain *ca.* 100 mg g^{-1} Re uptake under 0.5 mol kg^{-1} HNO_3 . It was even higher than the maximum

Table 2 Parameters of the adsorption of ReO_4^- onto $\text{PC}_2\text{-C}_{12}\text{vimBr-A}$ from the Langmuir model

Intercept, $1/q_m k$	Slope, $1/q_m$	R^2	q_m , (mg g^{-1})	K , (ppm^{-1})
0.02036	0.00179	0.9997	559	0.0879



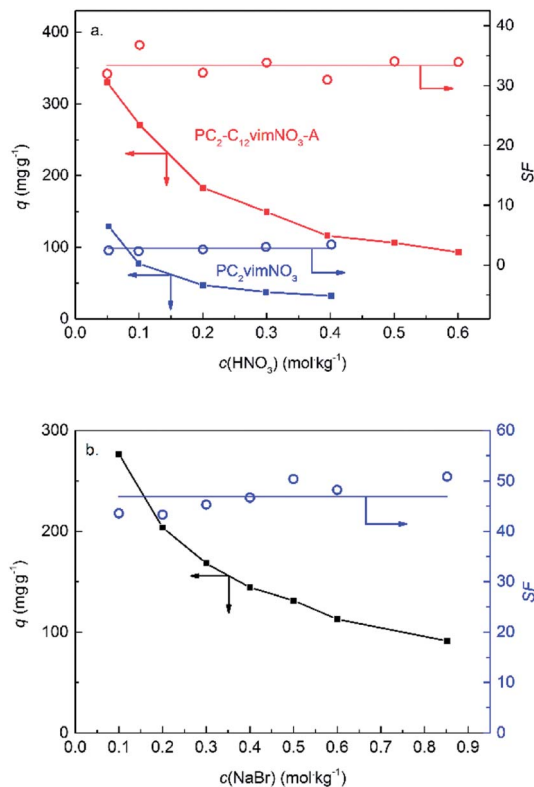


Fig. 5 (a) The competitive adsorption towards ReO_4^- against NO_3^- on $\text{PC}_2\text{-C}_{12}\text{vimNO}_3\text{-A}$ as well as on $\text{PC}_2\text{vimNO}_3$. (b) The competitive adsorption towards ReO_4^- against Br^- on $\text{PC}_2\text{-C}_{12}\text{vimBr-A}$. The c_0 was 700 ppm.

Table 3 The average values of the SF of $\text{PC}_2\text{-C}_{12}\text{vimNO}_3\text{-A}$, $\text{PC}_2\text{-vimNO}_3$ and $\text{PC}_2\text{-C}_{12}\text{vimBr-A}$ towards ReO_4^- against the corresponding competitors

Adsorbent	Competitor	SF
$\text{PC}_2\text{-C}_{12}\text{vimNO}_3\text{-A}$	NO_3^-	33.4 ± 1.9
$\text{PC}_2\text{vimNO}_3$	NO_3^-	2.8 ± 0.5
$\text{PC}_2\text{-C}_{12}\text{vimBr-A}$	Br^-	46.9 ± 3.1

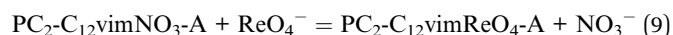
adsorption capacities of some other reported adsorbents.^{3,38} The potential practical usage of $\text{PC}_2\text{-C}_{12}\text{vimBr-A}$ for the treatment of radioactive liquid wastes was revealed by such high Re uptake under this condition. The SF of PC_2vimBr against Br^- was higher than that against NO_3^- , and it is agreed with the sequence of increasing hydration energies ($\text{ReO}_4^- < \text{NO}_3^- < \text{Br}^-$).³⁹

Varied contents of polar organic solvents in the mixed solvent could be used to investigate the effect of solvent on the adsorption.⁴⁰ And the lower hydration energy of ReO_4^- than those of the competitors was widely used for the selective adsorption or extraction of ReO_4^- .¹ Herein, ethanol was added in the solvent for illustrating the importance of water in the selective adsorption of ReO_4^- . As shown in Fig. 6, the q as well as the SF were decreased with the increasing ethanol content. With increasing ethanol content, the activity of water decreased,

thus the contribution of the differences of hydration energies to the selective adsorption was decreased for the system. So it could be concluded that water as a solvent played an important role in the selective adsorption of ReO_4^- onto $\text{PC}_2\text{-C}_{12}\text{vimNO}_3\text{-A}$ gel.

3.4 The adsorption thermodynamics of $\text{PC}_2\text{-C}_{12}\text{vimBr-A}$ towards ReO_4^-

The SF of $\text{PC}_2\text{-C}_{12}\text{vimNO}_3\text{-A}$ towards ReO_4^- against NO_3^- can be considered as the K of the following equation:



The K under different temperatures were measured, and the relation between $\ln K$ and $1000/T$ (Fig. 7) were fitted by the van't Hoff equation:

$$\ln K = -\frac{\Delta H^\ominus}{RT} + \frac{\Delta S^\ominus}{R} \quad (10)$$

The ΔH^\ominus and ΔS^\ominus of eqn (9) were calculated from the slope and the intercept, which were $-16.9 \text{ kJ mol}^{-1}$ and $29 \text{ J mol}^{-1} \text{ K}^{-1}$, respectively.

The negative ΔH^\ominus indicated that the adsorption process was exothermic, and lower temperature was beneficial to the adsorption process. The type of adsorption can be indicated by the magnitude of the enthalpy change value. Lower enthalpy change corresponds to physical adsorption, and higher one corresponds to chemical adsorption. The range of enthalpy change of physical adsorption is considered as $0\text{--}20 \text{ kJ mol}^{-1}$ (ref. 41) or $0.5\text{--}5 \text{ kcal mol}^{-1}$ ($2.1\text{--}20.9 \text{ kJ mol}^{-1}$).⁴² The absolute value of ΔH^\ominus of eqn (9) was in the range of enthalpy change of physical adsorption, so the adsorption process of $\text{PC}_2\text{-C}_{12}\text{vimNO}_3\text{-A}$ towards ReO_4^- was physical adsorption. This was agreed with the ion-exchange mechanism, where no covalent bond forms or breaks.

3.5 The adsorption cycles and the adsorption mechanism of $\text{PC}_2\text{-C}_{12}\text{vimBr-A}$ towards ReO_4^-

Though $\text{PC}_2\text{-C}_{12}\text{vimBr-A}$ had high adsorption selectivity towards ReO_4^- , ReO_4^- can be exchanged into solution by high

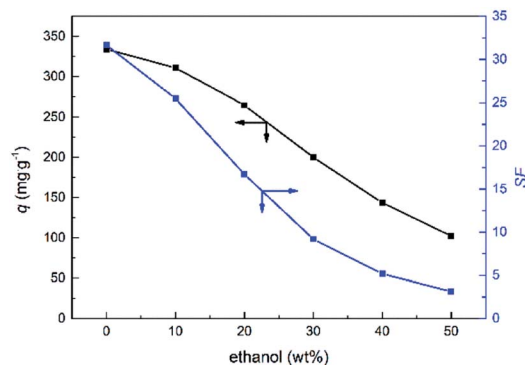


Fig. 6 The competitive adsorption towards ReO_4^- against NO_3^- on $\text{PC}_2\text{-C}_{12}\text{vimNO}_3\text{-A}$ in ethanol–water mix solvent. The c_0 was 700 ppm.



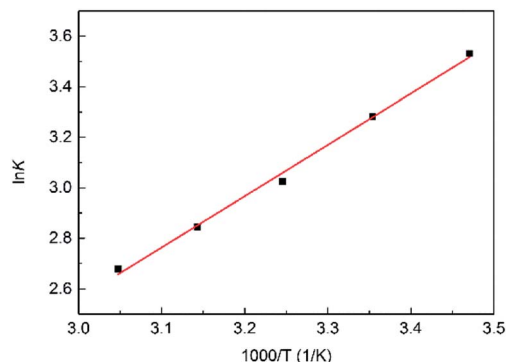


Fig. 7 Fitted curve of $\ln K-1000/T$ of eqn (9).

concentration NO_3^- . So the used adsorbent can be renewed by HNO_3 with high concentration resulting in the formation of $\text{PC}_2\text{-C}_{12}\text{vimNO}_3\text{-A}$. After washing off HNO_3 by deionized water, $\text{PC}_2\text{-C}_{12}\text{vimNO}_3\text{-A}$ can adsorb ReO_4^- again by anion-exchanging. The adsorption cycles of $\text{PC}_2\text{-C}_{12}\text{vimBr-A}$ towards ReO_4^- were shown in Fig. 8, where the Re uptake were marked by red and the Re desorbed in the first wash by 5.40 mol kg^{-1} HNO_3 were marked by blue.

The q in the second cycle was reduced to *ca.* 96% of that of the first cycle and kept well in the next two cycles. The decrease of q after the first cycle could be explained by the anion exchange from Br^- to NO_3^- after the first cycle. $\text{PC}_2\text{-C}_{12}\text{vimReO}_4\text{-A}$ could be renewed into $\text{PC}_2\text{-C}_{12}\text{vimNO}_3\text{-A}$ by HNO_3 and the adsorbent had excellent reusability. Most ReO_4^- could be desorbed in the first wash by 5.4 mol kg^{-1} NO_3^- , and the second wash could renew almost all the ion-exchange positions. The eluted Re in HNO_3 solution exists without any other salts, and can be made into Re products for other usages easily, or disposed separately from other wastes.

IR and XPS were performed to characterize $\text{PC}_2\text{-C}_{12}\text{vimBr-A}$, $\text{PC}_2\text{-C}_{12}\text{vimReO}_4\text{-A}$ and the $\text{PC}_2\text{-C}_{12}\text{vimNO}_3\text{-A}$ after desorption (Fig. 9).

As Br^- has no IR absorbance, the peaks of the polymeric imidazolium cation were revealed clearly in the IR spectrum of $\text{PC}_2\text{-C}_{12}\text{vimBr-A}$. After the adsorption of ReO_4^- , in the IR spectrum of $\text{PC}_2\text{-C}_{12}\text{vimReO}_4\text{-A}$, no change of the peaks of the polymeric imidazolium cation could be observed, and the peak

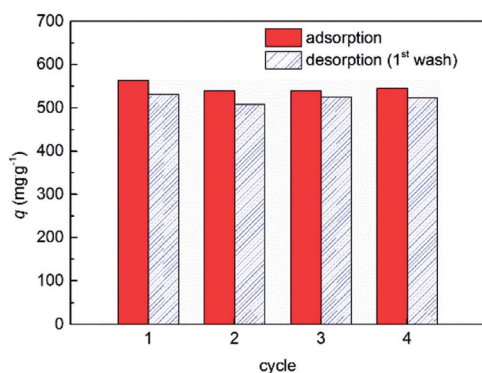


Fig. 8 The adsorption cycles of ReO_4^- on $\text{PC}_2\text{-C}_{12}\text{vimBr-A}$.

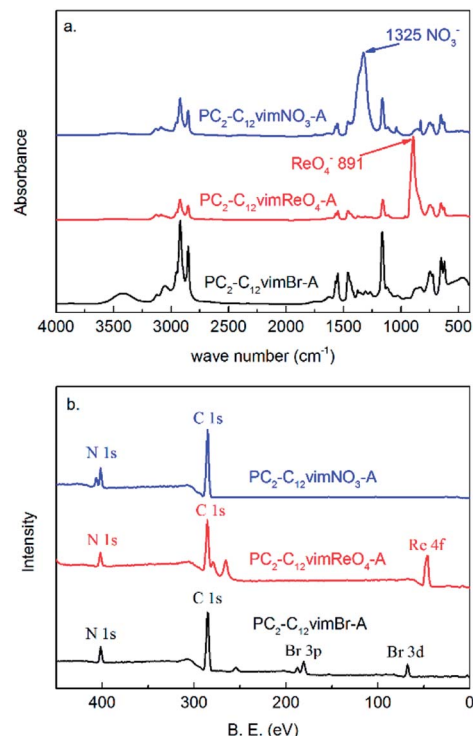


Fig. 9 The (a) IR and (b) XPS pattern of $\text{PC}_2\text{-C}_{12}\text{vimBr-A}$, $\text{PC}_2\text{-C}_{12}\text{vimReO}_4\text{-A}$ and the $\text{PC}_2\text{-C}_{12}\text{vimNO}_3\text{-A}$ after desorption.

of ReO_4^- at 891 cm^{-1} occurred. After the desorption by 5.4 mol kg^{-1} HNO_3 , the peak of ReO_4^- disappeared, and the strong peak of NO_3^- at 1325 cm^{-1} occurred, while the other peaks showed no change. It could be concluded from the IR spectra that the polymeric imidazolium cation did not change during the adsorption and the desorption process, and ReO_4^- and NO_3^- were exchanged onto the polycation without valence change. The XPS also confirmed the adsorption and the desorption was successful. The peak of Re occurred in $\text{PC}_2\text{-C}_{12}\text{vimReO}_4\text{-A}$ instead of that of Br in $\text{PC}_2\text{-C}_{12}\text{vimBr-A}$, and it disappeared in the XPS of $\text{PC}_2\text{-C}_{12}\text{vimNO}_3\text{-A}$ after desorption. The peak of N in $\text{PC}_2\text{-C}_{12}\text{vimNO}_3\text{-A}$ was a double peak, instead of the single peaks in $\text{PC}_2\text{-C}_{12}\text{vimBr-A}$ and $\text{PC}_2\text{-C}_{12}\text{vimReO}_4\text{-A}$, for the N in $\text{PC}_2\text{-C}_{12}\text{vimNO}_3\text{-A}$ could be divided into two kinds with different B.E., which belonged to NO_3^- and imidazolium respectively (see also Fig. S1†). So an ion-exchange mechanism could be concluded from the IR and the XPS results.

Furthermore, as an anion-exchange gel, $\text{PC}_2\text{-C}_{12}\text{vimBr}$ may be used for the adsorption of other anions, such as $\text{Cr}(\text{vi})$ anions, anionic surfactants and anionic dyes in the future.

4. Conclusions

Polymeric ionic liquid gels, $\text{PC}_2\text{-C}_{12}\text{vimBr}$, was synthesized by radiation-induced polymerization and crosslinking, and its adsorption behavior towards ReO_4^- was investigated. The $\text{PC}_2\text{-C}_{12}\text{vimBr}$ gel contained two kinds of imidazolium units, namely the hydrophilic units composed of ethylimidazolium and the hydrophobic units composed of dodecylimidazolium. Addition of small amount of hydrophilic units could effectively improve



the adsorption kinetics of PC₁₂vimBr gel, and the addition of hydrophobic units could improve the adsorption selectivity towards ReO₄[−] of PC₂vimBr gel. PC₂-C₁₂vimBr-A gel, with 20 mol% hydrophilic units and 80 mol% hydrophobic units, had an adsorption equilibrium time of *ca.* 24 h and adsorption capacity as high as 559 mg g^{−1} (mg Re per g gel). Its SF towards ReO₄[−] against NO₃[−] was 33.4 ± 1.9, which was more than 10 times of that of PC₂vimBr, and it could keep a Re uptake as high as 100 mg g^{−1} in 0.5 mol kg^{−1} HNO₃, which revealed its potential application in the treatment of Tc in radioactive liquid wastes. The adsorption mechanism was ion-exchange, and the selective adsorption was driven by the low hydration energy of ReO₄[−] and the hydrophobicity of the polycation. The ΔH^\ominus and ΔS^\ominus of the NO₃[−]/ReO₄[−] ion-exchange reaction of PC₂-C₁₂vimNO₃-A were −16.9 KJ mol^{−1} and 29 J mol^{−1} K^{−1}, respectively. The adsorbent could be renewed by 5.4 mol kg^{−1} HNO₃ for several times with high adsorption performance maintenance. The work provided a new approach to prepare novel ionic gel adsorbent by controlling the hydrophilicity and hydrophobicity of adsorbents which are related to the kinetics and selectivity towards adsorbates, respectively.

Conflicts of interest

There are no conflicts to declare.

Acknowledgements

The National Natural Science Foundation of China (NNSFC, Project No. 21471161 and 11375019) and the Scientific and Technological Plan of Shenzhen City (JCYJ 2015061616311759) are acknowledged for supporting this research.

Notes and references

- 1 D. Banerjee, D. Kim, M. J. Schweiger, A. A. Kruger and P. K. Thallapally, *Chem. Soc. Rev.*, 2016, **45**, 2724–2739.
- 2 S. Sarri, P. Misaelides, D. Zamboulis, X. Gaona, M. Altmaier and H. Geckeis, *J. Radioanal. Nucl. Chem.*, 2016, **307**, 681–689.
- 3 X. Shu, L. Shen, Y. Wei and D. Hua, *J. Mol. Liq.*, 2015, **211**, 621–627.
- 4 I. Yamagishi and M. Kubota, *J. Nucl. Sci. Technol.*, 1993, **30**, 717–719.
- 5 B. A. Lenell and Y. Arai, *J. Hazard. Mater.*, 2017, **321**, 335–343.
- 6 T. L. Yu, S. Q. Liu, M. Xu, J. Peng, J. Q. Li and M. L. Zhai, *Radiat. Phys. Chem.*, 2016, **125**, 94–101.
- 7 J. J. Neeway, R. M. Asmussen, A. R. Lawter, M. E. Bowden, W. W. Lukens, D. Sarma, B. J. Riley, M. G. Kanatzidis and N. P. Qafoku, *Chem. Mater.*, 2016, **28**, 3976–3983.
- 8 C. D. Williams and P. Carbone, *Environ. Sci. Technol.*, 2016, **50**, 3875–3881.
- 9 S. A. Wang, E. V. Alekseev, D. W. Juan, W. H. Casey, B. L. Phillips, W. Depmeier and T. E. Albrecht-Schmitt, *Angew. Chem., Int. Ed.*, 2010, **49**, 1057–1060.
- 10 S. A. Wang, P. Yu, B. A. Purse, M. J. Orta, J. Diwu, W. H. Casey, B. L. Phillips, E. V. Alekseev, W. Depmeier, D. T. Hobbs and T. E. Albrecht-Schmitt, *Adv. Funct. Mater.*, 2012, **22**, 2241–2250.
- 11 D. Banerjee, S. K. Elsaidi, B. Aguila, B. Li, D. Kim, M. J. Schweiger, A. A. Kruger, C. J. Doonan, S. Ma and P. K. Thallapally, *Chem.-Eur. J.*, 2016, **22**, 17581–17584.
- 12 D. Banerjee, W. Xu, Z. Nie, L. E. V. Johnson, C. Coghlan, M. L. Sushko, D. Kim, M. J. Schweiger, A. A. Kruger, C. J. Doonan and P. K. Thallapally, *Inorg. Chem.*, 2016, **55**, 8241–8243.
- 13 D. Sheng, L. Zhu, C. Xu, C. Xiao, Y. Wang, Y. Wang, L. Chen, J. Diwu, J. Chen, Z. Chai, T. E. Albrecht-Schmitt and S. Wang, *Environ. Sci. Technol.*, 2017, **51**, 3471–3479.
- 14 A. V. Desai, B. Manna, A. Karmakar, A. Sahu and S. K. Ghosh, *Angew. Chem., Int. Ed.*, 2016, **55**, 7811–7815.
- 15 H. Hu, B. Jiang, H. Wu, J. Zhang and X. Chen, *J. Environ. Radioact.*, 2016, **165**, 39–46.
- 16 H. Hu, B. Jiang, J. Zhang and X. Chen, *RSC Adv.*, 2015, **5**, 104769–104778.
- 17 P. Rajec, O. Rosskopfova, M. Galambos, V. Fristak, G. Soja, A. Dafnomili, F. Noli, A. Dukic and L. Matovic, *J. Radioanal. Nucl. Chem.*, 2016, **310**, 253–261.
- 18 P. Rajec, M. Galambos, M. Dano, O. Rosskopfova, M. Caplovicova, P. Hudec, M. Hornacek, I. Novak, D. Berek and L. Caplovic, *J. Radioanal. Nucl. Chem.*, 2015, **303**, 277–286.
- 19 W. R. Wilmarth, G. J. Lumetta, M. E. Johnson, M. R. Poirier, M. C. Thompson, P. C. Suggs and N. P. Machara, *Solvent Extr. Ion Exch.*, 2011, **29**, 1–48.
- 20 C. Nash, B. Musall, M. Morse and D. McCabe, *Sep. Sci. Technol.*, 2015, **50**, 2881–2887.
- 21 P. Xiao, D. Han, M. L. Zhai, L. Xu and H. B. Li, *J. Hazard. Mater.*, 2017, **324**, 711–723.
- 22 J.-H. Zu, Y.-Z. Wei, M.-S. Ye, F.-D. Tang, L.-F. He and R.-Q. Liu, *Nucl. Sci. Tech.*, 2015, **26**, 69–75.
- 23 B. Gierczyk, M. Ceglowski and M. Zalas, *PLoS One*, 2015, **10**, e0122891.
- 24 D. Han, X. Li, J. Peng, L. Xu, J. Li, H. Li and M. Zhai, *RSC Adv.*, 2016, **6**, 69052–69059.
- 25 J. Zu, M. Ye, P. Wang, F. Tang and L. He, *RSC Adv.*, 2016, **6**, 18868–18873.
- 26 W. Luo, A. Inoue, T. Hirajima and K. Sasaki, *Appl. Surf. Sci.*, 2017, **394**, 431–439.
- 27 M. Petrova, M. Guigue, L. Venault, P. Moisy and P. Hesemann, *Phys. Chem. Chem. Phys.*, 2015, **17**, 10182–10188.
- 28 B. H. Gu, G. M. Brown, P. V. Bonnesen, L. Y. Liang, B. A. Moyer, R. Ober and S. D. Alexandratos, *Environ. Sci. Technol.*, 2000, **34**, 1075–1080.
- 29 D. Jermakowicz-Bartkowiak and B. N. Kolarz, *React. Funct. Polym.*, 2011, **71**, 95–103.
- 30 D. Pan, G. Ye, F. Wang and J. Chen, *Prog. Chem.*, 2012, **24**, 2167–2176.
- 31 S. Tachimori, S. Suzuki and Y. Sasaki, *J. At. Energy Soc. Jpn.*, 2001, **43**, 1235–1241.
- 32 J. Y. Yuan, D. Mecerreyes and M. Antonietti, *Prog. Polym. Sci.*, 2013, **38**, 1009–1036.
- 33 J. Y. Yuan and M. Antonietti, *Polymer*, 2011, **52**, 1469–1482.



- 34 L. C. Tome and I. M. Marrucho, *Chem. Soc. Rev.*, 2016, **45**, 2785–2824.
- 35 Y. Jiang, F. Li, G. Ding, Y. Chen, Y. Liu, Y. Hong, P. Liu, X. Qi and L. Ni, *J. Colloid Interface Sci.*, 2015, **455**, 125–133.
- 36 Z. Dong, J. Z. Liu, W. J. Yuan, Y. P. Yi and L. Zhao, *Chem. Eng. J.*, 2016, **283**, 504–513.
- 37 J. Chen, Y. Y. Ao, T. R. Lin, X. Yang, J. Peng, W. Huang, J. Q. Li and M. L. Zhai, *Polymer*, 2016, **87**, 73–80.
- 38 S. Milicevic, L. Matovic, D. Petrovic, A. Aukic, V. Milosevic, D. Dokic and K. Kumric, *J. Radioanal. Nucl. Chem.*, 2016, **310**, 805–815.
- 39 J. Behnsen and B. Riebe, *Appl. Geochem.*, 2008, **23**, 2746–2752.
- 40 R. Konasova, J. J. Dytrtova and V. Kasicka, *J. Sep. Sci.*, 2016, **39**, 4429–4438.
- 41 H. Demey, T. Vincent, M. Ruiz, A. M. Sastre and E. Guibal, *Chem. Eng. J.*, 2014, **244**, 576–586.
- 42 D. Liping, S. Yingying, S. Hua, W. Xinting and Z. Xiaobin, *J. Hazard. Mater.*, 2007, **143**, 220–225.

